JOURNAL OF Materials CHEMISTRY

# Nano-SnSb alloy deposited on MCMB as an anode material for lithium ion batteries

**Lihong Shi, Hong Li, Zhaoxiang Wang, Xuejie Huang and Liquan Chen***

*Laboratory for Solid State Ionics, Institute of Physics, Chinese Academy of Sciences, Beijing 100080, China. E-mail: lqchen@aphy02.iphy.ac.cn; Fax: +86-10-82649351*

***Received 12th December 2000, Accepted 8th March 2001***
***First published as an Advance Article on the web 2nd April 2001***

Nanosized SnSb alloy has been deposited and dispersed uniformly on the surface of mesophase carbon microbeads (MCMB) by a co-precipitation method in glycerin solution. As an active anode material for lithium ion batteries these composites show improved cycling performance. This improvement is due to the dispersion of the nano-sized alloy particles on the carbon surface that can alleviate the aggregation of nano-sized alloy particles during Li insertion and extraction. Furthermore, as both SnSb alloy and MCMB are active materials for Li-storage, a higher reversible capacity of 420 mA h $g^{-1}$ has been achieved for the composite containing 26 wt% of SnSb alloy deposited on MCMB.

## Introduction

Much effort has been made since the 1980s to study alloy-based anode materials for lithium rechargeable batteries due to their high Li-storage capacities.[1,2] However, a serious problem for alloy materials with large particle sizes is rapid pulverization during discharge and charge cycles. In order to improve their structural stability, superfine alloy, intermetallic compounds and active/inactive composite alloy materials, such as Sn/$SnSb_x$, Sn/$SnAg_x$, SnFe/SnFeC and nano-Si/C have been investigated.[2–10] In general, active materials with small particles are supposed to have less observable volume variation and keep a rather stable microstructure during cycling.[3,7] For intermetallic compounds as well as active/inactive composite materials, the active component is formed *in situ* and uniformly dispersed in the inactive matrix at the atomic or nanometer scale, similar to that in the oxide anodes.[6] As a result, the volume variation of the active component could be alleviated effectively and the cyclic performance of superfine alloy anodes is improved impressively. Furthermore, nanosized materials have also shown significant advantages in kinetics.[8]

However, it was found in our recent studies that when the particle size of an active material is less than 100 nm, the particles, such as SnSb, Si, Ag and Sb, always aggregate severely and merge into micrometer-scale particles during Li insertion and extraction.[11–13] The aggregation leads to significant volume changes in the electrode and a gradual decline of the electrochemical capacity. In addition, the kinetic advantage of nanosized materials disappears. The aggregation can be hindered partly by mixing a large amount of dispersant such as carbon black with the active material.[11] However, it is very difficult for the dispersant to prevent nano-particles from aggregating completely unless a very large proportion of dispersant is added. In fact, particle aggregation has been observed in nano-silicon electrodes even though carbon black was added with an equal weight of the active material.[12] On the other hand, the introduction of the electrochemically inactive dispersant or matrix leads to a decrease of the volumetric capacity of the electrode.

In this paper we propose to deposit a nanosized alloy on the surface of carbonaceous particles with large diameters. If the nano-SnSb alloy particles cannot contact with each other, aggregation may be prevented. Based on this proposal, a series of nano-SnSb/MCMB composite materials has been prepared. Their electrochemical performances as anode materials for Li ion batteries have been investigated. Attention was also paid to the morphology variation of the alloy particles.

## Experimental

The preparation of the nano-SnSb alloy deposited on MCMB is similar to that for nanosized β-SnSb alloy.[14] In brief, $SbCl_3$ and $SnCl_2{\cdot}H_2O$ (99%, AR, Beijing Chemical Reagent) were mixed with a molar ratio of 5 : 4 and dissolved in glycerin (99%, AR, Beijing Chemical Reagent) to form a 0.5 M solution. Then MCMB powder with an average particle size of 10 μm (Anshan, China) was added into the solution. The mixture was cooled to 0.0–1.0 °C. Zinc powder (99.9%, 250 mesh, AR, Beijing Chemical Reagent Company) in a 95% stoichiometric amount was added into the solution slowly and stirred continually at the same time. Finally, the product was washed with ethanol and filtered before being dried in a vacuum at 55 °C. A series of composite materials with different weight percentages of nano-SnSb were prepared and named as CNSS1, CNSS2, CNSS3, CNSS4 and CNSS5. The nominal and actual compositions of these samples according to chemical analysis are listed in Table 1.

X-Ray powder diffraction (XRD) was carried out on a Rigaku B/max-2400 X-ray diffractometer with Cu-Kα radiation. The morphology of the nano-SnSb coated MCMB was investigated with a Hitachi S-4000 scanning electron microscope. The transfer of Li-inserted electrodes into the vacuum chamber before SEM investigation was protected by argon atmosphere, which is similar to our previous method.[12]

The preparation of the electrodes and the assembly of the electrochemical cells were described in our previous report.[14] MCMB coated with nanosized SnSb alloy was used as the

**Table 1** Nominal and actual compositions of samples

| | Nominal composition | | | Actual composition | | |
|---|---|---|---|---|---|---|
| Sample | Sn (wt%) | Sb (wt%) | SnSb (wt%) | Sn (wt%) | Sb (wt%) | SnSb (wt%) |
| CNSS1 | 8.76 | 11.24 | 20 | 8.20 | 8.69 | 16.89 |
| CNSS2 | 13.14 | 16.86 | 30 | 9.70 | 16.4 | 26.15 |
| CNSS3 | 17.52 | 22.48 | 40 | 13.0 | 19.4 | 32.4 |
| CNSS4 | 21.9 | 28.1 | 50 | 18.5 | 24.8 | 43.3 |
| CNSS5 | 26.28 | 33.72 | 60 | 21.4 | 30.0 | 51.4 |

 DOI: 10.1039/b009907o

**This journal is © The Royal Society of Chemistry 2001**

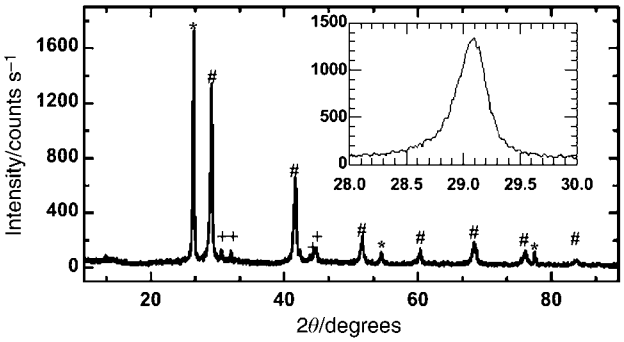


**Fig. 1** XRD pattern of MCMB coated with 26% weight of nanosized SnSb alloy (CNSS2). *: graphite phase; #: β-SnSb; +: β-Sn. Inset figure is the profile of the (012) rhombohedral line.

working electrode and metallic Li foil as the counter electrode. The weight ratio of the active material to binder polyvinylidene fluoride (PVDF) in the working electrode is 95 : 5. 1 M $LiPF_6$ dissolved in EC–DEC (1 : 1 in volume) was used as the electrolyte. The cells were discharged and recharged at a current density of 0.2 mA cm$^{-2}$ between 2.0 and 0.0 V.

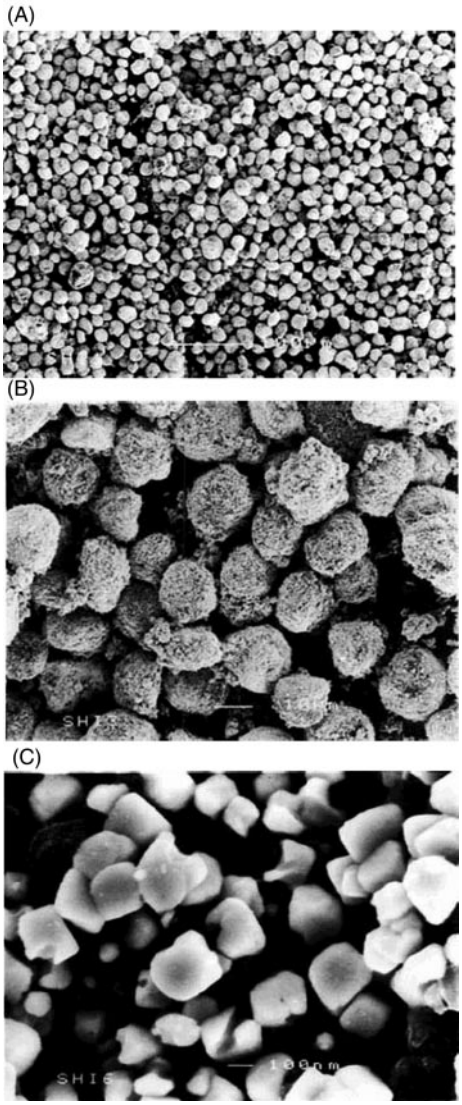


**Fig. 2** The SEM images of MCMB coated with 26% weight of nanosized SnSb alloy: (A) white bar = 100 μm, (B) white bar = 10 μm, (C) white bar = 100 nm.

## Results and discussion

A typical XRD pattern (sample CNSS2) is shown in Fig. 1. The peaks marked with "#" are attributed to the rhombohedral β-SnSb phase. According to the feature in the inset figure, various Sb-rich alloy phases in addition to the pure Sb phase are not distinguished.[15,16] Therefore, this sample consists of pure β-SnSb ($x_{Sb} = 0.6$). The peaks denoted "*" are related to the graphitic structure of MCMB. The other weak peaks demonstrate the presence of metallic Sn in the composite. The particle size of β-SnSb is estimated to be about 25 nm based on the Scherrer formula.

Typical SEM images of CNSS2 are shown in Fig. 2(A), (B) and (C) at different magnification levels. It can be seen from Fig. 2(A) that most of the nano-SnSb alloy particles were deposited on the surface of MCMB and dispersed uniformly as shown in Fig. 2(B) and (C). There are also a few free SnSb particles in the sample. The amount of disassociated nano-SnSb particles increases with the nano-SnSb content in the composite materials, especially over 30 wt%. Compared with the morphology of pure nano-SnSb alloy samples, which were prepared in similar procedures without the addition of MCMB,[14] the particle size of the SnSb alloy in the composite materials is reduced to 100 nm. This indicates that the alloy particles are composed of small grains. Moreover, the dendrite morphology of the pure SnSb alloy is not observed in the composite material. It is significant that MCMB particles provide many surface active sites for the nucleation of the SnSb alloy so that the alloy particles are dispersed on the surface of MCMB uniformly and cannot grow adequately to form

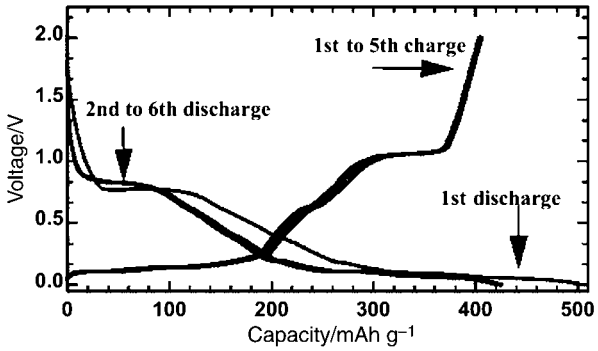


**Fig. 3** The discharge–charge curves of a CNSS2 anode in a lithium battery: CNSS2/1 M $LiPF_6$, EC–DEC (1 : 1, v/v)/Li. Current density = 0.2 mA cm$^{-2}$.

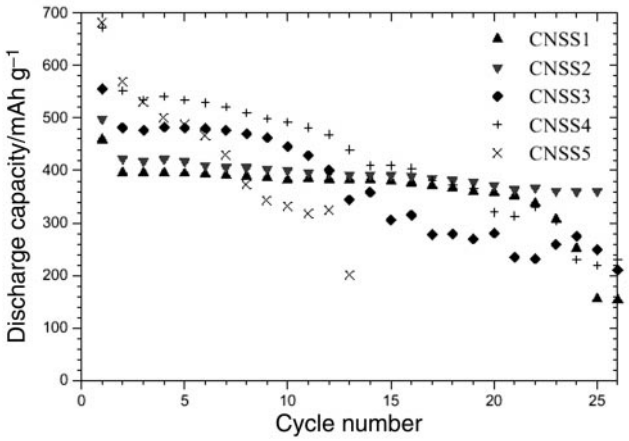


**Fig. 4** The cyclic performance for the series of CNSS$x$ materials used as active anode materials in lithium ion batteries: CNSS$x$/1 M $LiPF_6$, EC–DEC (1 : 1, v/v)/Li. Current density = 0.2 mA cm$^{-2}$.

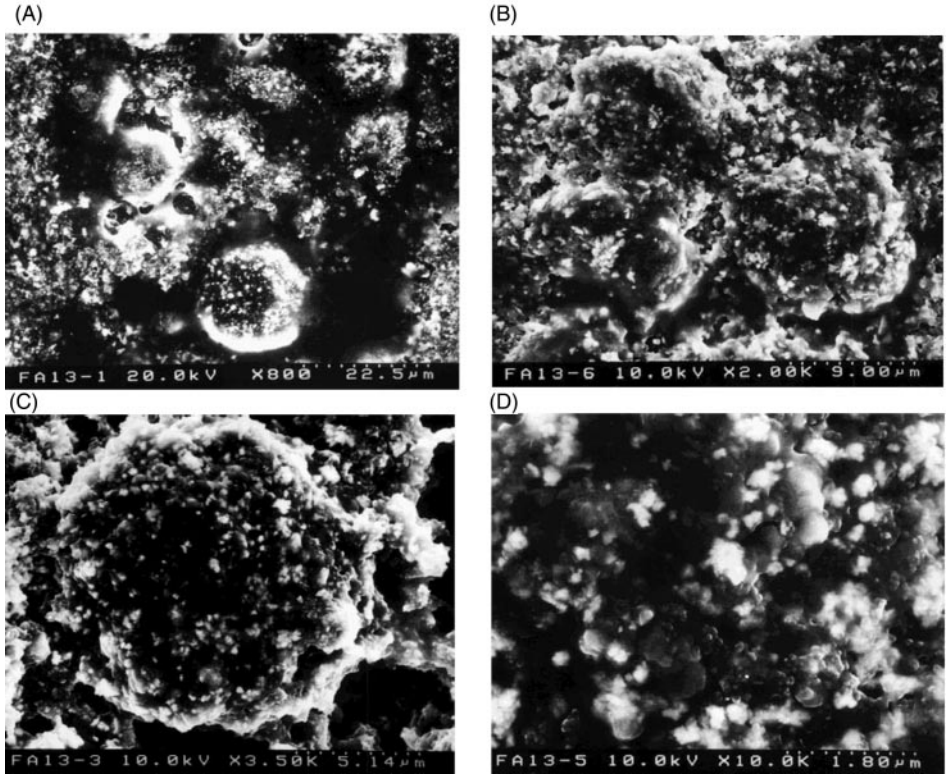


**Fig. 5** The SEM images of CNSS2 after several discharge and charge cycles in a lithium ion battery. (A) The scale is 22.5 μm. The bright region like a film in the left middle region is produced by the destructive effect of electron beam focusing. (B) The scale is 9 μm. Three connected MCMB particles are visible. (C) The scale is 5.14 μm. A MCMB particle is visible. (D) The scale is 1.8 μm. The surface of a MCMB particle is shown.

dendritic structures under similar reaction conditions. The influence of the surface properties of MCMB on the particle size, morphology and distribution of the nano-SnSb alloy will be studied further.

The discharge and charge curves of a CNSS2/Li cell are shown in Fig. 3 as an example. During Li insertion, Li–Sb and Li–Sn alloys are formed successively in the voltage range of 0.9–0.2 V[14] while the intercalation reaction of Li ions into the interlayers of the crystal lattice of MCMB occurs mainly below 0.2 V. Significantly, both the alloy reactions and the intercalation reactions are reversible. The reversible capacity for CNSS2 is as high as 420 mA h $g^{-1}$. The voltage profiles for the other samples are similar to that of CNSS2 but the capacity ratio of alloy reaction and Li intercalation reaction is different depending on the weight percentage of SnSb alloy in the composite material. Compared with pure nano-SnSb alloy and nano-SnSb alloy with 20 wt% carbon black,[11,14] the reversibility of the alloy reaction for the composite materials consisting of nano-SnSb deposited on MCMB with a weight ratio of SnSb alloy lower than 30% is much better as seen in Fig. 4. Considering the capacity and cyclic capability, the optimal weight ratio for SnSb alloy is between 20% and 30%.

The discharge and charge efficiency for CNSS2 in the first cycle is 85%. The value is a little higher than the calculated value of 81% (nano-SnSb, 67%; MCMB, 92%). We have found that the well-known solid electrolyte interphase layer (SEI) is also present on the surface of nano-SnSb particles during discharge/charge cycles.[11] The formation of the SEI layer contributes to the significant irreversible capacity loss in the first cycle. It is reasonable to assume that the surface area of the alloy/carbon composite material exposed to the electrolyte is smaller than the sum of the surface areas of nano-SnSb and MCMB. This may lead to the decrease of the irreversible capacity.

Fig. 5 shows the SEM images of a CNSS2 electrode after several charge and discharge cycles. It is obvious that most of the SnSb particles on the surface of MCMB remain separated. However, neighboring MCMB balls are connected through SnSb alloy particles. Therefore, those nano-SnSb particles which are disassociated or occupy the adjacent sites between two MCMB balls can merge together. Owing to the large

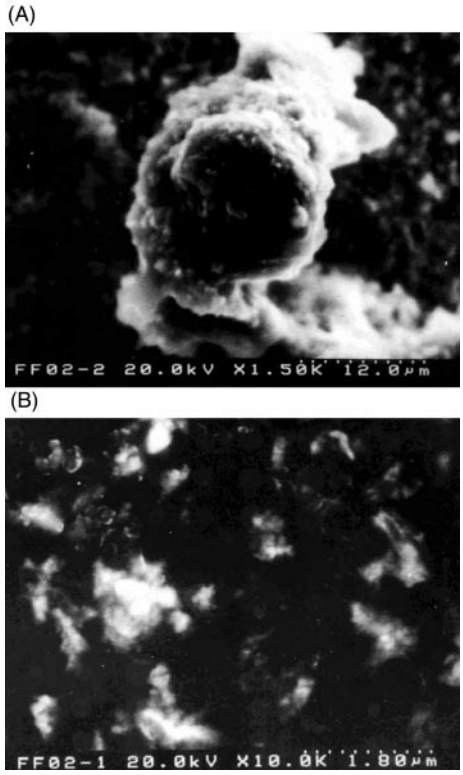


**Fig. 6** The SEM images of CNSS4 after several discharge and charge cycles in a lithium ion battery. (A) The scale is 12 μm. A protruded MCMB particle on the aggregation bodies is visible. (B) The scale is 1.8 μm. The surface of the particle is shown.

particle size of MCMB in comparison to SnSb, most of the SnSb particles on the surface of MCMB are not expected to form aggregates. In fact, even if the nano-SnSb alloy particles in the interface regions are merged together, the size of the aggregate is still quite small due to the very small amount of free SnSb alloy particles. In addition, the aggregation bodies can keep better electric contact with each other due to the rather high electronic conductivity of the core MCMB. Consequently, the cyclic performances of CNSS1 and CNSS2 are much better. When the content of SnSb alloy is beyond a critical value, the amount of disassociated SnSb alloy particles increases significantly. In that case, the surface of MCMB cannot act as an efficient dispersant to separate the alloy particles. The aggregation becomes very severe as shown in Fig. 6. Most of the carbon particles are covered with a connected and densely aggregated layer. In this figure, only one of the MCMB particles is protruded and can be seen. Others are embedded into the aggregates.

The above results indicate that if nanosized alloy particles can be dispersed on the surface of a rigid ball with large particle size, the aggregation can be alleviated significantly and their cyclic performance can be improved impressively. This proposal provides many possibilities for preparing new anode materials to meet different demands for lithium ion batteries, such as controlled potential profile, high capacity, high volume specific capacity, high rate performance and so on. Further work is still in progress.

## Conclusions

A composite material in which nanosized alloy particles are deposited onto the surface of carbon materials with larger particle size is prepared by a co-precipitation method. The composite materials can alleviate the aggregation of nanosized alloy particles effectively during electrochemical cycling if the weight ratio of SnSb alloy is less than 30%. As a result, the cyclic performance of the composite materials is improved impressively and a reversible capacity as high as 420 mA h $g^{-1}$ is obtained. When the weight ratio of SnSb alloy exceeds 30%, MCMB can no longer prevent the nano-SnSb alloy from aggregating. As a result, their capacity fades quickly although their initial reversible capacity is very high.

## Acknowledgements

This work is supported by NSFC (contract No. 59972041) and National 863 key program.

## References

1 B. A. Boukamp, G. C. Lesh and R. A. Huggins, *J. Electrochem. Soc.*, 1981, **128**, 725.
2 R. A. Huggins, *Solid State Ionics*, 1998, **113**, 57.
3 J. Yang, M. Winter and J. O. Besenhard, *Solid State Ionics*, 1996, **90**, 281.
4 O. Mao, R. A. Dunlap, I. A. Courtney and J. R. Dahn, *J. Electrochem. Soc.*, 1998, **145**, 4195.
5 K. D. Kepler, Jj. T. Vaughey and M. M. Thackery, *Electrochem. Solid State Lett.*, 1999, **2**, 307.
6 O. Mao, R. L. Turner, I. A. Courtney, B. D. Fredericksen, M. I. Buckett, L. J. Krause and J. R. Dahn, *Electrochem. Solid State Lett.*, 1999, **2**, 3.
7 J. Yang, M. Wachtler, M. Winters and J. O. Besenhard, *Electrochem. Solid State Lett.*, 1999, **2**, 161.
8 H. Li, X. J. Huang, L. Q. Chen, Z. G. Wu and Y. Liang, *Electrochem. Solid State Lett.*, 1999, **2**, 547.
9 H. Kim, J. Choi, H. Sohn and T. Kang, *J. Electrochem. Soc.*, 1999, **146**, 4401.
10 R. A. Huggins, *J. Power Sources*, 1999, **81–82**, 13.
11 H. Li, L. H. Shi, W. Lu, X. J. Huang and L. Q. Chen, *J. Electrochem. Soc.*, 2001, in press.
12 H. Li, X. J. Huang, L. Q. Chen, G. W. Zhou, Z. Zhang and D. P. Yu, *Solid State Ionics*, 2000, **135–137**, 181.
13 X. D. Wu, H. Li, X. J. Huang and L. Q. Chen, in *Proceedings of the 7th Asian Conference on Solid State Ionics*, ed. B. Chowdari and Wenji Wang, World Scientific Press, Singapore, 2000, p. 493.
14 H. Li, G. Y. Zhu, X. J. Huang and L. Q. Chen, *J. Mater. Chem*, 2000, **10**, 693.
15 V. Vassiliev, M. Lelaurain and J. Hertz, *J. Alloys Compds.*, 1997, **247**, 223.
16 JCPDS, 33-0118.